DEPARTMENT OF THE INTERIOR
U.S. GEOLOGICAL SURVEY

MISCELLANEOUS FIELD STUDIES
MAP MF-1465-C
PAMPHLET

MAP SHOWING QUATERNARY AND PLIOCENE FAULTS IN THE SILVER CITY 1°x2° QUADRANGLE AND THE DOUGLAS 1°x2° QUADRANGLE, SOUTHEASTERN ARIZONA AND SOUTHWESTERN NEW MEXICO

By

Michael N. Machette and Stephen F. Personius, U.S. Geological Survey;
Christopher M. Menges, University of New Mexico;
Philip A. Pearthree, University of Arizona and
Arizona Bureau of Mines and Mineral Technology

1986

INTRODUCTION

This is the third map in a series being compiled at a scale of 1:250,000 to show known and inferred Pliocene and Quaternary faults in the Rio Grande rift and Basin and Range Province in New Mexico, western Texas, and southeastern Arizona (see index map). The map and this pamphlet show amounts of vertical offset (throw), age of faulted deposits, time of last fault movement (table 2 on accompanying map), and data on the morphology of fault scarps (figs. 6-12 and table 3 in this pamphlet), as well as the distribution of Pliocene to Quaternary sediments and volcanic rocks, and pre-Pliocene rocks in the area.

Although previous small-scale maps of the Rio Grande rift (Woodward and others, 1975; Hawley, 1978; Baldridge and others, 1983) show many of the features depicted in this map series, the series is the first to focus specifically on neotectonic features (such as faults and folds) whose latest movement occurred in the past 5 Ma (millions of years). This report describes 22 of the most prominent faults in the area and discusses their history of movement.

The most recent faulting in the southeastern part of the Basin and Range Province and the whole Rio Grande rift occurred in 1887, just south of the map area in northernmost Mexico. This faulting is associated with a long fault zone that extends north into the United States along the eastern side of the San Bernardino Valley in Arizona.

Our studies indicate that Holocene (<10,000 yrs) and latest Pleistocene (10,000-25,000 yrs ago) movement may have occurred along five discrete faults (or fault zones) in the map area. These faults commonly lie along the margins of basins that have a generally north-south trend in the southern half of the map area (south of Interstate Highway 10). The remainder of the young faults in the area show evidence of late Pleistocene to Pliocene movement, and those north of I-10 lie along northwest-trending basins and ranges. This difference in orientation may be due to a possible regional 30° clockwise rotation of the least-principal-stress axis in the past 30 Ma (Machette and Colman, 1983) that has influenced the modern extensional tectonic setting of the area. Although we have no conclusive data, Quaternary faults in the northern part of the map area may have an oblique component of slip owing to east-west extension on pre-existing, predominantly northwest-southeast-trending faults.

Data used to compile this map come from published and unpublished geologic maps and literature, inspection of aerial photographs, and limited field investigation of Quaternary faults and their scarps. The sources of geologic data are quite variable, ranging from reconnaissance maps at scales of 1:62,500 or smaller to detailed maps at scales of 1:24,000 or larger. Amounts of offset were determined in three general ways: (1) from field measurements of net offset of surfaces across the fault, (2) from measurements from aerial photographs and from 1:24,000-scale topographic maps, and (3) from published data, which are sparse. The field measurements are probably accurate to within 10 percent of the amount of surface offset. Measurements from maps and aerial photographs are less accurate and are shown as ranges of estimated offsets along the length of a fault (for example, 5-20 m of surface offset).

Only those faults that displace, or are inferred to displace, Pliocene or younger materials are shown on this map, and many more young faults may be present than are shown. Because Pliocene or younger faulting probably occurred but cannot be demonstated or dated in many areas that have only Miocene or older rocks, most faults in these areas are not shown. In other areas, deposition or erosion may have concealed or removed evidence of young faulting. Also, young faults may not have a surface expression where the underlying basin-fill sediment is dissected or where surficial deposits are not present. Thus, our approach of showing only faults having known or suspected movement produces a map having a conservative number of faults. Readers using this map for hazards assessment, regional analyses of structural patterns, or

similar studies should be aware that many other young faults could be, and probably are, present in Miocene and older rocks in the map area.

GEOLOGIC SETTING AND NEOTECTONIC HISTORY

The pre-Pliocene geology of the area is briefly discussed here because many neotectonic features are controlled by older structures. Recent reports pertinent to the late Cenozoic geologic history of southeastern Arizona and southwestern New Mexico include discussions of the structural evolution of the Rio Grande rift in New Mexico (Chapin and Seager, 1975; Chapin, 1979), the geology of the Silver City 1°x2° quadrangle by Drewes and others (1982), potassium-argon age determinations on basalt and the late Cenozoic geologic history of the southern rift by Seager and others (1984), and guidebooks to southwestern New Mexico (edited by Fitzsimmons and Lockman-Balk, 1965), southeastern Arizona (edited by Callender and others, 1978), and the Rio Grande rift of New Mexico and Colorado (compiled by Hawley, 1978).

Although some geologists disagree about the details of the Cenozoic structural evolution of the southwestern United States, a three-phase history of Cenozoic extension has been gaining acceptance, particularly for the Arizona part of the Basin and Range Province (Menges, 1981; Menges and others, 1981). These phases include (1) a post-Laramide, middle Tertiary (Oligocene to middle Miocene) orogeny characterized by relatively ductile extension (low-angle normal faulting during the late stages of development of metamorphic core complexes) and calc-alkaline volcanism; (2) a transition period (middle Miocene); and (3) the classic Basin-and-Range-style disturbance (late Miocene to present) characterized by brittle, high-angle extensional block faulting and basaltic to bimodal volcanism (Shafiqullah and others, 1976, 1978). For other views on the history and style of Cenozoic deformation, see summaries by Loring (1976), Drewes (1981), and Seager and others (1984).

The Basin-and-Range-style faults (phase 3; late Miocene to recent) appear to be superposed on, and(or) controlled by, (1) a preexisting terrane of northwest-trending Laramide-age folds and thrust (or reverse) faults (see Davis, 1979; Drewes, 1978, 1981), and (2) a complex terrane of early to middle Tertiary normal faults formed prior to inception of Basin-and-Range-style faulting. The northwest trend of young faults in the northern part of the map area may be strongly controlled by these preexisting structural trends (Elston and others, 1976; Deal and others, 1978), but in the southern part of the map area young faults have a more northerly trend.

The change from middle Tertiary ductile extension and widespread calc-alkaline magmatism to late Tertiary block faulting and basaltic-bimodal volcanism occurred over a transition period of relative quiescence, although both mechanisms remained active (Shafiqullah and others, 1980; Elston, 1981; Seager and others, 1984). Evidence for this transitional phase includes regional unconformities between syntectonic units and changes in style of faulting and volcanism. Region-wide unconformities that separate middle Tertiary syntectonic sedimentary rocks from younger sediments are between 12 and 17 Ma (Damon and others, 1973; Eberly and Stanley, 1978; Shafiqullah and others, 1980). The presence of these unconformities suggests a major change in tectonic style during the transition period. In addition, there is strong evidence in the Rio Grande rift and southern Basin and Range Province for a dramatic rotation of the least-principal-stress direction in the past 30 Ma. In this region Pliocene and Quaternary faults, dikes, and volcanic vents generally are oriented north-south (Machette and Colman, 1983), whereas early to middle Miocene faults and volcanic features commonly trend northwest (Coney, 1978; Davis, 1981; Lipman, 1981, 1983; Menges, 1981; Menges and others, 1981; Aldrich and Laughlin, 1982; Laughlin and others, 1983). These data, as well as analyses by Zoback and Zoback (1980) and Zoback and others (1981), suggested to Machette and Colman (1983) that the orientation of the least-principle-stress axis may have rotated as much as 30° clockwise during the late Tertiary.

In southeastern Arizona, the late Tertiary Basin-and-Range-style disturbance, which began about 11-15 Ma, is characterized by generally high-angle, planar normal faults that bound symmetric to strongly asymmetric horsts, grabens, and half grabens (Aiken and Sumner, 1974; Aiken, 1978; Eberly and Stanley, 1978; Scarborough and Pierce, 1978; Shafiqullah and others, 1980; Menges, 1981). Onset of Basin-and-Range-style faulting was accompanied by a change in regional patterns of volcanism. Widespread sequences of silicic ash-flow deposits emplaced during the middle Tertiary were succeeded by generally dispersed, locally voluminous eruptions of alkali basalt and bimodal assemblages of basalt and rhyolite (McKee and Anderson, 1971; Deal and others, 1978; Shafiqullah and others, 1980; Suneson and Luchitta, 1983). The late Tertiary volcanism is different from earlier, middle Tertiary volcanism in its eruptive style, geochemistry, and more restricted distribution.

Because basalt is commonly intruded along deep faults that may not have surface expression, the map shows the distribution of extrusive features and extrusive rocks (commonly basalt in this region) of less than 5 Ma in age. Most of the young dated volcanic rocks in the map area are of late Pliocene and Pleistocene age (3.3-0.3 Ma, table 1 on accompanying map). These rocks form flows, pyroclastic agglutinate cones, sparse tuff rings, and maar craters; they are concentrated in a large field in the San Bernardino Valley of southeastern Arizona, but several isolated flows and vents are present about 25 km to the northeast in the

central Animas Valley of southwestern New Mexico.

In the map area, the middle to late Cenozoic stratigraphic record contains several sedimentary units that range from Oligocene to Pliocene in age. These deposits are products of various depositional and deformational environments. Heindl (1958, 1962a, 1962b) noted that the Gila Conglomerate of Gilbert (1875), which traditionally has been the most frequently used term for the alluvial basin fill in the area, spans most of the late Cenozoic. To date, only a few local sedimentary sequences have been studied enough to warrant new formation names, owing to correlation problems that arise from local patterns of sedimentation and the general absence of regional marker horizons or precise age control. However, a stratigraphic break is present in many places between the little-deformed upper Tertiary basin fill and the older tilted, indurated, and more lithologically diverse middle Tertiary sedimentary rocks. In most cases, the basin-fill unit on the map is restricted to young sediments (upper or Pliocene part of the Gila Conglomerate) as defined by Scarborough and Pierce (1978), although uniform differentiation of these units throughout the map area currently is not feasible.

A total of 1,000-3,000 m of clastic basin-fill sediment (Gila Conglomerate) now fills grabens formed during the Basin-and-Range-style disturbance (Scarborough and Pierce, 1978). These deposits are generally subdivided into two major units on an informal basis: syntectonic, lower basin fill (mostly Miocene) that commonly is in fault contact with bedrock along the basin margins and late- to post-tectonic, largely undeformed upper basin fill (latest Miocene and Pliocene to middle Pleistocene) that overlaps some range-bounding faults (Scarborough and Pierce, 1978; Menges and McFadden, 1981). However, both parts of the Gila Conglomerate are less deformed than the older and strongly deformed middle Tertiary sedimentary rocks.

The largely undeformed upper part of the Gila Conglomerate is probably 6-3 Ma (Johnson and others, 1975; Scarborough, 1975; Lindsay, 1978; Dickson and Izett, 1981; Menges, 1981; Menges and McFadden, 1981). This age range indicates that major Basin-and-Range-style faulting declined during the late Miocene and eventually ceased in many basins by the middle Pliocene (Menges, 1981; Menges and McFadden, 1981). In addition, these rocks overlap extensive (2- to more than 7-km-wide) pediments that flank many of the ranges in the region. The presence of extensive pediments and lack of evidence of faulting in much of the Pliocene and Pleistocene section implies that much of the offset on Basin-and-Range-style faults occurred in the late Miocene (15-6 Ma), rather than in the Pliocene and Quaternary.

Although stratigraphic evidence indicates that faulting in most of the region had slowed or ceased by middle Pliocene time, faulting in some areas persisted well into the Quaternary. In particular, the San Bernardino, San Simon, and Animas Valleys are active grabens characterized by scattered late Quaternary basaltic volcanism and young faults.

The late Cenozoic history of the area has been dominated by nontectonic processes such as changes in climate during the Quaternary and progressive integration of formerly closed basin drainages into a regional network (Menges and McFadden, 1981). The early part of this history is marked by a gradual decrease in rate and amount of deposition of basin fill. In many basins, basin-fill deposition probably ended in latest Pliocene or early Pleistocene time (2.5-1.0 Ma) and was succeeded by deposition of relatively thin, coarser grained units of surficial material associated with alluvial-fan complexes (such as fans on Frye Mesa and the fan of John Long Canyon in the Safford and Sulphur Springs Valleys, respectively). These fans commonly form subregional geomorphic surfaces, and their deposits lie on extensive pediments and basin-wide erosion surfaces cut with slight angular unconformity across the upper basin fill. Most of the large fans and associated surfaces extend undisturbed across range-bounding faults. The fans probably record the fluvial response to the onset of a wetter Pleistocene climate (Melton, 1965; Menges and McFadden, 1981). In contrast, terrace and piedmont gravel deposits inset at progressively lower levels in most basins of the map area were deposited in response to climatic fluctuations during the Pleistocene. Progressive integration of local drainage systems with the Gila River drainage system in the Pliocene-Pleistocene triggered 100-300 m of dissection in many basins in the western part of the map area. Deposition has continued throughout the Quaternary in those basins that are still closed, such as the Sulphur Springs and Animas Valleys.

METHODS FOR DETERMINING TIME OF FAULTING

Two methods were used in this study to determine the time of most-recent faulting. The first method is a stratigraphic approach by which the time of the most recent faulting is bracketed between the ages of the youngest faulted and oldest unfaulted deposits. Recurrent fault movement is recognized by comparing the cumulative amount of displacement in deposits of various ages. The second method of estimating ages of undated fault scarps is by comparing their morphology with the morphology of dated scarps.

STRATIGRAPHIC METHODS

Map units that are keyed to a refined stratigraphic assemblage provide age control for determining the time of faulting. In the map area, the distribution of young basin-fill and surficial deposits, young volcanic rocks, and some young faults were taken from maps by Dane

and Bachman (1961), Morrison (1965), Thorman and Drewes (1978), Drewes (1980), Drewes and Thorman (1980a, 1980b), and Drewes and others (1982). Their mapping was supplemented by reconnaissance of aerial photographs.

Surficial and young basin-fill deposits are here divided into four categories to help classify age of fault movement (fig. 1). The oldest category, Pliocene to early Pleistocene (ep, 5.0-0.75 Ma), includes basalt and interbedded sedimentary rocks of the San Bernardino and Animas volcanic fields and the upper part of the Gila Conglomerate. The next younger categories, middle Pleistocene (mp, 750-150 ka) and late Pleistocene (lp, 150-10 ka), include surficial deposits that form terraces, piedmont slopes, and alluvial fans, as well as young basalt flows of the San Bernardino and Animas volcanic fields. The youngest category, Holocene (h, 0-10 ka), includes alluvium of the lowest terraces and modern flood plains, the youngest alluvial-fan deposits, playa sediments, and thin deposits of eolian sand.

FAULT-SCARP MORPHOLOGY

Stratigraphy and relative-dating techniques provide the chronologic framework for the Quaternary and Pliocene deposits that record faulting. However, the faulting may be considerably younger than the deposits that are affected. Analysis of fault-scarp degradation has given us a new tool that is appropriate for both reconnaissance and detailed investigations of faulting. Using easily made profiles of normal-fault scarps, morphometric data is used to determine the time elapsed since their formation. The basis of this technique is simple: for two scarps of comparable height and material (for example, a sandy gravel), the older scarp is the one having the more subdued topography, in terms of both slope and curvature. Calibration for determining the age of faulting comes from scarps and similar geomorphic features (shorelines and fluvial-terrace scarps) that are dated stratigraphically. This approach dates the earthquake itself, rather than a geomorphic surface or stratigraphic layer that provides only maximum limits on time of last movement.

The approach used here is based on Bucknam and Anderson's (1979) empirical relation between the height of a fault scarp (H) and its maximum scarp-slope angle (θ), which followed the results of Wallace's (1977) studies of slope-degradation processes and the morphology of fault scarps. The scarp-morphology data presented in the following discussion show the relation between fault-scarp height and maximum scarp-slope angle, the variation of these two parameters, and their relation to fault scarps of known age. Our studies are based on the following premises of fault-scarp evolution: (1) initially, the free face of the fault scarp is nearly vertical, reflecting the near-surface dip of the fault; (2) the face soon slumps to the angle of repose of the faulted material, typically 32°-35° for unconsolidated surficial deposits; and (3) the slope of the scarp then decreases at a slower rate, mainly by the process of slopewash (Wallace, 1977; Nash, 1981). We have analyzed only those fault scarps on unconsolidated deposits, primarily of Quaternary age. Most of the fault scarps studied are on pebbly sand to sandy gravel alluvium, material that is generally of the same texture as scarps studied by Bucknam and Anderson (1979).

Age category and range	Age symbol	Description of geologic units
Holocene (0-10 ka)	h	Modern alluvium in channels and on floodplains, eolian sand, and young playa and alluvial-fan deposits.
Late Pleistocene (10-150 ka; latest Pleistocene, 10-25 ka)	lp	Alluvial deposits that form terraces, piedmont slopes, and fans. Also includes young basalt flows of local extent.
Middle Pleistocene (150-750 ka)	mp	Alluvial deposits that form terraces, piedmont slopes, and fans. Locally includes uppermost part of basin-fill deposits in undissected basins and young basalt flows.
Early Pleistocene (750 ka to 2 Ma) and Pliocene (2-5 Ma)	ep	Upper basin-fill deposits (Gila Conglomerate) and locally interbedded basalt flows.

Figure 1.--Age categories and symbols for surficial deposits and upper part of basin-fill deposits in map area.

Scarp nomenclature and measurement of scarp profiles

The heights of fault scarps were determined from detailed topographic surveys made along traverses perpendicular to the scarps. We used a vernier-scale hand level and Jacobs staff, cloth tape, and stadia rod to measure slope angles across the scarp. These traverses extended 20-100 m above and below the fault scarp to determine the slopes of the adjacent alluvial surfaces. Measurements were made at intervals of 2-5 m on the upper and lower slopes and at intervals of 0.5-2 m on the scarp itself.

The nomenclature used in this report is modified only slightly from that used by Bucknam and Anderson (1979). Scarp height (H, in meters; fig. 2) is the vertical distance between the surfaces above and below the scarp where intersected by the plane representing the maximum scarp-slope angle (θ). The angles θ and γ denote the inclination from horizontal of the scarp and the adjacent land surfaces, respectively. The maximum scarp-slope angle was measured over a length equal to 10-20 percent of the distance between the crest and toe of the scarp at four to six locations within 3-5 m of each traverse line. The values of θ reported here are the averages of the repeated measurements. Thus, each traverse yielded a scarp profile and each profile yielded a value for H and θ (a data pair).

At least seven data pairs are needed for statistical analysis. Data sets smaller than seven may or may not represent the morphology of a fault scarp accurately; however, these smaller data sets still are useful to show local variation in height and steepness along the length of a fault scarp.

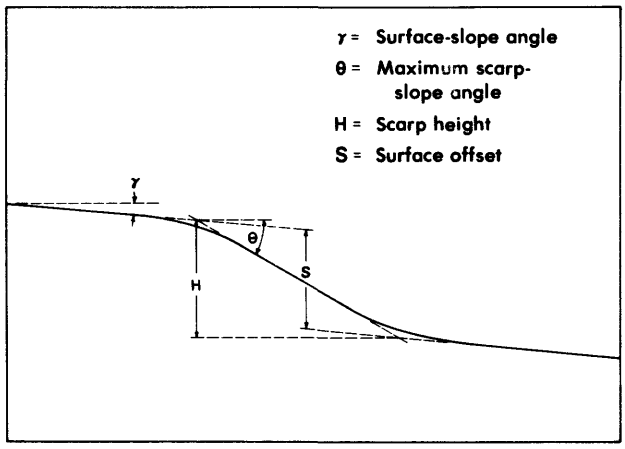

Figure 2.--Diagrammatic profile of a hypothetical fault-scarp (modified from Bucknam and Anderson, 1979, fig. 1).

We measured the height and maximum scarp-slope angle of an individual scarp at several places along its length. Most heights range from about 1 to 10 m, but some older scarps are as much as 20 m high. We chose sites we judged to be relatively stable, avoiding areas of active erosion or deposition. Some parts of the map area have an extensive cover of eolian sand that renders large tracts of ground unsuitable for studies of fault-scarp morphology. Discontinuous, en echelon, or segmented scarps (segments are sections of faults that each have a discrete history of surface rupture), were treated as individual scarps.

Major factors that affect the rate of scarp degradation include the texture and cohesion of the faulted deposits, orientation of the scarp, and the climate, vegetation, biologic activity, and topographic relief at the scarp site. We chose profiling sites where these characteristics were as uniform as possible so that observed differences in scarp morphology would largely reflect the age of a scarp. Although variations exist between some scarps, especially in the texture of the faulted deposits, the measurements presented here represent typical fault scarps in the area.

Relation between maximum scarp-slope angle and scarp height

The studies of Bucknam and Anderson (1979) showed that the heights of scarps (H) of a given age correlate with their maximum scarp-slope angle (θ, fig. 3). The relation holds for a wide range of heights and slope angles and also applies to fluvial scarps and wave-cut shorelines, such as those formed during the highest stand of Lake Bonneville in Utah. Although the Lake Bonneville shoreline escarpment is an erosional feature, Bucknam and Anderson (1979) consider that it eroded much like a fault scarp. The main difference in these two genetically different features is that a fault scarp requires an initial time interval for the free face to collapse to the angle of repose, whereas a shoreline escarpment probably has an initial scarp-slope angle that is equal to, or slightly less than, the angle of repose (instead of nearly vertical). The time required for the scarp to degrade in such a manner has not been determined, but the degree of erosion of historic scarps in the Basin and Range Province suggests to us that this interval is not more than a thousand years.

The empirical relation used here is based on a least-squares linear regression equation of the form $\theta=a+b(\log H)$ (where a is the value of θ when H=1 m and b is the slope of the line). Bucknam and Anderson (1979) found that 91 percent of the variation in the two parameters for the Bonneville shoreline is explained by the equation, $\theta=3.8+21.0(\log H)$ (Bucknam, 1980). They also found that scarps younger and older than the Bonneville shoreline have similar

relations, but plot in respectively higher and lower parts of the graph of θ versus H. The presentation of scarp-morphology data in this report follows the style of Bucknam and Anderson (1979) as illustrated in figure 3, which shows data from a hypothetical fault scarp. In this and other, similar figures data points are shown as filled circles and, where seven or more data pairs were obtained, the equation for the line of best fit and the coefficient of determination (R^2) are included.

We noted three conditions for which H and θ do not correlate. The first involves fault scarps having maximum scarp-slope angles (θ) that are only a few degrees steeper than the adjoining land surfaces; such scarps generally have a weak correlation between H and θ and a low value for b. The second involves scarps formed by offset of surfaces having gradients (Y, fig. 3) of more than about 5°. In such cases, the scarp can be anomalously steep (and this relation yields an erroneously young age). The third involves young scarps having slope angles that exceed the angle of repose of the faulted material. In this case, the relation will apply only to small scarps that have slopes less than the angle of repose, whereas the large scarps will have slope angles that cluster about the angle of repose.

The methods and results of Bucknam and Anderson (1979) and Machette and McGimsey (1983) were used to assign relative ages to fault scarps. For calibration we used the lines of best fit for data from two scarps of known age

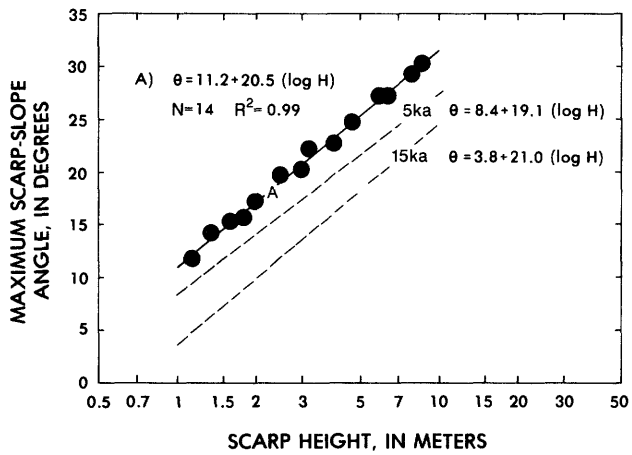

Figure 3.--Maximum scarp-slope angle (θ) plotted against scarp height (H) for a hypothetical fault scarp. Also shown are the number of data pairs (n), the coefficient of determination (R^2), and two reference lines for age comparisons (5 ka--Cox Ranch and La Jencia faults; 15 ka--Bonneville shoreline) and corresponding equations for the lines of best fit.

t shown in figure 3. This figure (and a si... presentation in fig. 5) is the basis for comparison of scarp data throughout this report. The uppermost dashed line (labeled 5 ka in figs. 3 and 5) represents data from segment C of La Jencia fault near Magdalena, N. Mex. (most recent movement about 5 ka; Machette and McGimsey, 1983; Machette, 1986). The second dashed line (labeled 15 ka in figs. 3 and 5) is based on Bucknam's (1980) data from the highest wave-cut shoreline of Lake Bonneville, Utah, which is here considered to have formed about 15 ka on the basis of stratigraphic and radiometric studies by Scott and others (1983).

We chose the following relatively conservative criteria to assign relative ages to fault scarps: scarps having (1) lines of best fit that lie above the upper dashed line on figure 3 (5 ka) are considered to be of Holocene age (less than 10 ka); (2) lines of best fit that lie between the two dashed lines indicate scarps of Holocene or latest Pleistocene age (less than 25 ka); and (3) lines of best fit that lie to the right of and below the lower dashed line (15 ka) indicate scarps of late Pleistocene age (10-150 ka) or, less likely, of middle Pleistocene age (150-750 ka).

COMPOUND FAULT SCARPS

Some fault scarps in the map area were formed by more than one episode of faulting as shown by either increasing scarp heights (Hm, fig. 4) in progressively older deposits or by scarps that have discrete facets--that is, compound-slope angles (Wallace, 1977). These compound scarps commonly have the form of degraded fault scarps that have been reactivated one or more times (the older scarp surfaces are denoted by the angle θ', fig. 4). We interpret many of the compound scarps by assuming that the steepest element of the scarp (θ and Hs, fig. 4) was formed during the most recent episode of faulting and that the remaining portion of the scarp (Hm minus Hs) represents previous faulting. In this case, Hs is defined as the difference in elevation between the old scarp surfaces where intersected by the plane of the maximum slope. A plot of Hs versus θ for a compound scarp and a plot of H versus θ for a single-event scarp along the same fault commonly will yield similar relations. When treated in such a manner, compound fault scarps yield values for Hs versus θ (open circles in fig. 5) that plot considerably younger than the data for Hm versus θ (filled circles in fig. 5). Note that the resultant lines of best fit for the youngest element of the scarps (Hs) commonly have steeper slopes (larger value for b in the regression equation) than do the data for the whole compound fault (Hm); also the former b values usually are similar to those of single-event scarps. From these relations it seems reasonable to assume that fault-scarp data represented by a line of best fit having a low

b value might indicate multiple episodes of faulting even though the scarp may not have obviously compound slope angles.

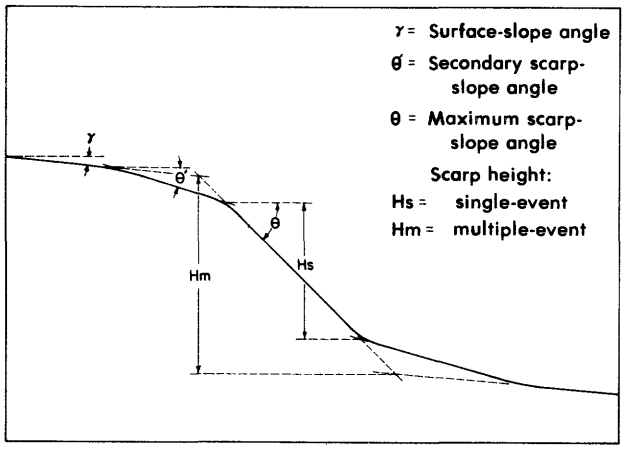

Figure 4.--Diagrammatic profile of a hypothetical compound fault scarp.

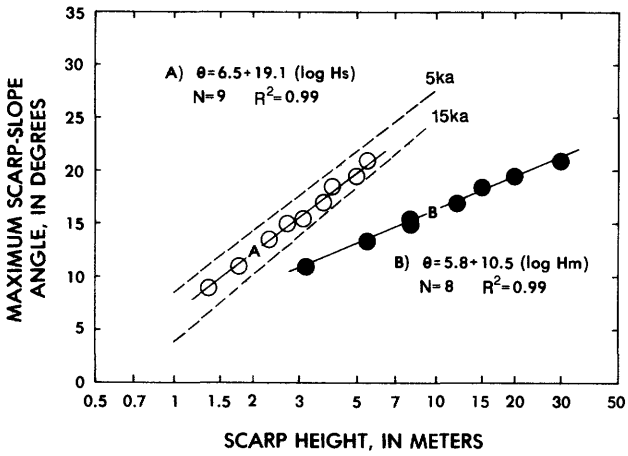

Figure 5.--Maximum scarp-slope angle (θ) plotted against scarp heights (Hs: open circles and line A; Hm: filled circles and line B) for a hypothetical compound fault scarp. Also shown are the number of data pairs (n), the coefficient of determination (R^2), two reference lines for age comparisons--5 ka and 15 ka--and corresponding equations for the lines of best fit.

EXAMPLES OF FAULT BEHAVIOR AND HISTORY

The following examples show how patterns of surface rupture, amounts of surface offset, and ages of faulted deposits can be used to decipher the timing of movement on a particular fault or fault zone.

SCARPS PRODUCED BY A SINGLE EPISODE OF MOVEMENT

Fault scarps produced by a single surface rupture or a combination of ruptures closely spaced in time (here referred to as a single episode of faulting) typically are of similar height in deposits of different ages. The following example shows a fault as it could appear on the accompanying map; in fact, many young fault scarps in the Rio Grande rift and Basin and Range Province have similar histories of movement and patterns of offset.

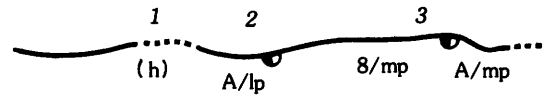

1. Deposits of Holocene age (h) are not offset.
2. Deposits of late Pleistocene age (lp) are offset less than 5 m (A).
3. Deposits of middle Pleistocene age (mp) are offset from less than 5 m (A) to as much as 8 m.

This example indicates that the faulting occurred in the late Pleistocene because the fault displaces upper Pleistocene deposits, but does not displace Holocene deposits. Although the amount of offset varies along the length of the fault, the scarp is probably the product of a single episode of movement. Secondly, because the amounts of offset in deposits of both late and middle Pleistocene age are similar, this fault scarp probably was formed during the late Pleistocene, as shown by a half-filled semicircle on the downdropped side of the fault.

SCARPS PRODUCED BY RECURRENT MOVEMENT ON A FAULT

Where scarps on old deposits are higher than those in young deposits recurrent movement is indicated on the fault. The following example shows a displacement pattern resulting from recurrent fault movement. Many faults that cut middle Pleistocene and older deposits in the Rio Grande rift show evidence of recurrent movement.

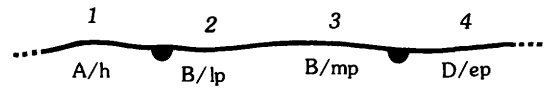

1. Deposits of Holocene age (h) are offset less than 5 m (A).
2. Deposits of late Pleistocene age (lp) are displaced 5-20 m (B).
3. Deposits of middle Pleistocene age (mp) also are offset 5-20 m.
4. Deposits of early Pleistocene to Pliocene age (ep) are offset 50-150 m (D).

This example indicates recurrent post-Pliocene movement because deposits of decreasing age are offset decreasing amounts, the last displacement being Holocene, as designated by a filled semicircle on the downthrown side of the fault. Additional evidence of Holocene movement might come from data on the scarp's morphology (see morphometric data in section below entitled "Prominent Quaternary Faults").

SCARPS PRODUCED BY MOVEMENT ON SEGMENTS OF A FAULT

Many fault scarps occur in segments distinguished by differing amounts of displacement, which express different times and histories of movement. The segments are commonly separated by unbroken ground, by en echelon steps, or by changes in the trend of the fault scarp. The following example shows a segmented fault that has nearly equal amounts of surface offset along its length but markedly different ages of movement on separate segments, as determined by fault-scarp morphology or other dating techniques. Without knowledge of time of movement along the individual fault segments, such a fault might be interpreted as having been formed by a single episode of movement,

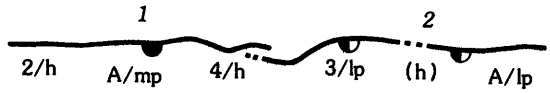

1. Along one segment of the fault, deposits of Holocene age (h) and middle Pleistocene age (mp) are offset similar amounts (2 m, 4m, and less than 5 m, respectively).
2. Along another segment of the fault, late Pleistocene deposits (lp) are offset less than 5 m (A), whereas intervening Holocene deposits (h) are not displaced.

The example indicates that the most recent faulting was Holocene along the first segment of the fault but was late Pleistocene along the second segment (shown by half-filled semicircles). This example is modeled after La Jencia fault in central New Mexico, where detailed trench investigations coupled with fault-scarp morphology (Machette and McGimsey, 1983) confirmed that different segments moved at different times and that the resultant scarps can vary widely in morphology along a single fault or fault zone.

PROMINENT QUATERNARY FAULTS

The following descriptions of Quaternary faults is based mostly on field studies in 1980-82 by C. M. Menges, P. A. Pearthree, and S. S. Calvo in Arizona and southwestern New Mexico and in 1980-81 by M. N. Machette in southwestern New Mexico. Previously unnamed faults are given informal names to facilitate discussion in the text; all faults are keyed by name and number to the accompanying map. Pertinent data for the faults are summarized in table 2 on the accompanying map and in table 3 and plots of scarp-morphology data (figs. 6-12) in this pamphlet.

Most of the ages of faulted surficial deposits mentioned in this section and shown on the accompanying map have been estimated (within broad ranges) from age-dependent criteria such as preservation of landform, degree and density of dissection, stratigraphic and topographic position, and soil development (see Birkeland, 1984, for a discussion of age-dating criteria and methods).

CACTUS FLAT FAULTS (1)

The faults on Cactus Flat are a series of normal faults that show minor offset in roadcuts of U.S. Highway 666, 3 km south of Safford, Ariz., first noticed by J. C. Witcher (oral commun., 1981). We find that the faults trend northwest and dip steeply northeast offsetting upper Pliocene to lower middle Pleistocene upper basin-fill deposits and terrace gravels of the Gila River. The terrace gravels, which are offset less than 0.5 m, are distinguished from the basin fill by the presence of distinctive red granitic clasts derived from a small area near Clifton, Ariz., 50 km northeast of Safford. The faulted Gila River terraces are overlain by undisturbed upper middle Pleistocene to upper Pleistocene piedmont-slope gravel derived from the Pinaleño Mountains southwest of the faults. These relations suggest that the youngest movement on the Cactus Flat faults was in middle Pleistocene time.

Although these faults lack topographic expression because of their small offset and antiquity, their surface traces generally coincide with stream and vegetation lineaments visible on aerial photographs. Other lineaments in the area suggest that intrabasin faults of middle Pleistocene age may be relatively abundant in the Safford area. However, the lack of late Pleistocene or Holocene faulting in the area indicates that faulting may have stopped or may have just shifted southward to the North and South Safford faults (3, 4).

BUENA VISTA FAULT (2)

The Buena Vista fault forms en echelon west-facing scarps about 2 km long on middle Pleistocene piedmont-slope alluvium about 5 km south of Buena Vista, Ariz. The scarps generally parallel the Gila River (3 km north), which suggests that they could be fluvial. Although the scarps are only 3 km from the Gila River, the lithology of the offset deposits indicates that the scarps represent faulting and not terrace erosion. The scarps are as much as 6 m high and have maximum scarp-slope angles of only 5°-9°. These relations suggest that the scarps are late Pleistocene or slightly older, and their morphology indicates only a single time of movement.

NORTH AND SOUTH SAFFORD FAULT ZONES (3, 4)

The North Safford (3) and South Safford (4) fault zones form a discontinuous series of east- to northeast-facing scarps that extend for 30 km along the east side of the Pinaleño Mountains, south of Safford, Ariz. The scarps were noted by Swan (1976) and J. C. Witcher (oral commun., 1980-1981) and were mapped during this study. The South Safford fault zone trends northwest across a pediment 2.5-4 km wide that is cut on Precambrian granite. The North Safford fault zone trends generally north along the front of the Pinaleños. Between these two segments, the widely dissected terrain and discontinuous fault scarps suggest that if the intervening section is a fault, it is less active than the adjacent fault segments.

Along the North Safford fault zone, compound fault scarps averaging 3.3 m in height are developed on middle Pleistocene deposits. These scarps are about the same height as those on middle Pleistocene deposits along the South Safford fault zone. Along the northernmost part of the North Safford fault zone, offset of lower(?) to lower middle-Pleistocene alluvium as much as 6-7 m suggests previous fault movements during early middle-Pleistocene time. Stratigraphic evidence of the most recent movement along the fault zone is less restricting because upper Pleistocene deposits are not present; however, middle Holocene deposits are undisturbed along major streams.

Scarp-morphology data from the North Safford fault zone (fig. 6) clearly suggest a slightly younger apparent age than scarp data from the South Safford fault zone (fig. 7), although the data show considerable scatter. The North Safford scarps are formed on coarse-grained, resistant alluvium, whereas the South Safford scarps are formed on less resistant sandy alluvium. This difference in texture may make the North Safford scarps more resistent to erosion and, thus, seem younger than the South Safford scarps.

Along the South Safford fault zone, alluvial deposits of latest Pleistocene age (10-20 ka) are offset an average of 1.1 m, but middle Pleistocene deposits are offset an average of 2.7 m. The offset pattern indicates about 1.6 m of faulting after deposition of the middle Pleistocene alluvium but before deposition of the uppermost Pleistocene alluvium. Our studies of scarp morphology suggest that the most recent movement is clearly pre-Holocene (fig. 7) and most probably latest Pleistocene. Stratigraphic evidence also suggests a pre-Holocene age for the fault, because middle(?) to upper Holocene alluvium is found undisturbed in major streams that cross the fault.

The stratigraphic evidence common to both the North and South Safford fault zones (similar offset in middle Pleistocene deposits, unfaulted Holocene deposits) suggests similar histories of movement since the middle Pleistocene. The most recent movement along the entire 30-km length of the two fault zones probably occurred in the latest Pleistocene, although nonsynchronous movement along the two zones cannot be ruled out.

In addition to the main scarps, two northeast-trending escarpments 10-25 m high are formed in alluvium of unknown age between the two fault zones. The relation (if any) of these possible fault scarps to the North and South Safford fault zones is unknown.

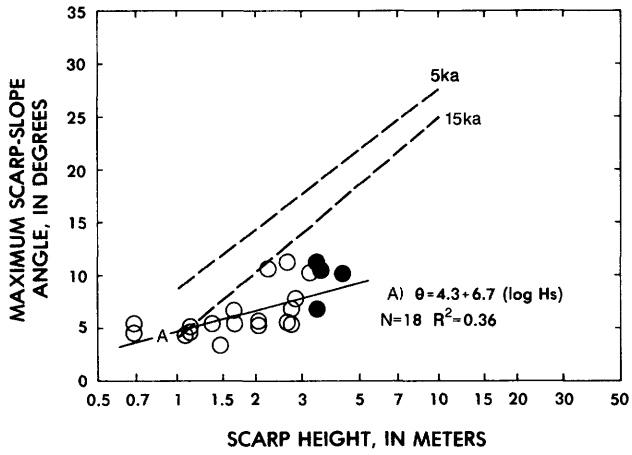

Figure 6.--Maximum scarp-slope angle (θ) plotted against scarp heights (Hs and Hm) for the North Safford fault zone (fault 3 on accompanying map). Open circles (line A) and regression equation are for most recent single-event part of scarp; filled circles are for entire multiple-event scarp.

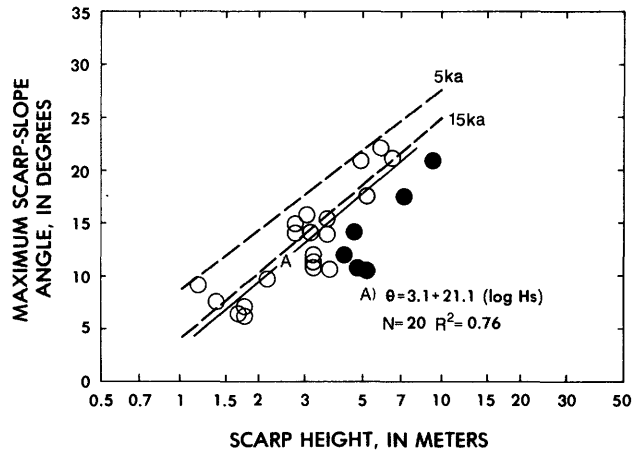

Figure 7.--Maximum scarp-slope angle (θ) plotted against scarp heights (Hs and Hm) for the South Safford fault zone (fault 4 on accompanying map). Open circles (line A) and regression equation are for most recent single-event part of scarp; filled circles are for entire multiple-event scarp.

WARD CANYON AND MAVERICK HILL FAULTS (5, 6)

The Ward Canyon (5) and Maverick Hill (6) faults form a set of Quaternary(?) fault scarps along the northeast side of the Duncan basin in the extreme north-central part of the map area. Cunningham's (1979) mapping and W. C. Witcher (1980; oral commun., 1980-1981) suggested that the scarps may be faults and our field reconnaissance confirms this suggestion. Although there are many suspected and known faults in the Duncan basin, we collected field data only on the Ward Canyon (5), Maverick Hill (6), and Rimrock (7) faults in the southern and central parts of the basin. The Rimrock fault is discussed separately in the following section.

The Ward Canyon fault forms a series of 10- to 20-m-high scarps that extend 15 km from 6.5 km northeast of Three Way, Ariz., to just east of Clifton, Ariz. (north of the map area). The scarps face southwest and disrupt topographically high, deeply dissected lower(?) Pleistocene alluvium. The fault itself is well exposed in Ward Canyon (east of Clifton and north of map area), where it has placed weakly consolidated upper Cenozoic deposits (on the west) against granitic bedrock. The time of the most recent movement, however, is not well dated in Ward Canyon. Southeast of Ward Canyon within the map area, the latest movement on the fault is middle Pleistocene or older because middle(?) and upper Pleistocene terrace alluvium is undisturbed by the fault.

The Maverick Hill fault, about 3 km east of the Ward Canyon fault, is also marked by a 12-km-long series of scarps 10-20 m high that disrupt deeply dissected lower Pleistocene alluvium. The fault has not been studied in detail, but is thought to be the same age as the Ward Canyon scarps, judging from similarities in morphology and amount of offset.

RIMROCK FAULT (7)

The Rimrock fault is one of several Quaternary faults that mark the eastern margin of the Duncan basin, 8 km northeast of Duncan, Ariz. All of the faults trend northwest and dip southwest. Scarps along the fault are on topographically high, lower to middle Pleistocene alluvium and are as much as 13 m high. A small asymmetric graben (not shown on the map) is present on middle to upper Pleistocene terrace alluvium, which is inset into the older, higher deposits; and scarps 1-2 m high that bound the west edge of the graben are buried by middle(?) to upper Holocene alluvium. The scarps have not been studied carefully, but their overall morphology suggests a late Pleistocene age.

PEARSON MESA FAULTS (8)

Pearson Mesa is a high piedmont surface along the southeast rim of the Duncan basin. About 15 km southeast of Duncan, the mesa is offset by two northeast-trending faults, both marked by northwest-facing scarps 5 km long and 5-6 m high. Backtilting of the piedmont slope between the two scarps has reversed the northwest gradient of the mesa, thus forming a small playa between the faults. We agree with Morrison (1965) that the Pearson Mesa scarps were formed by faulting. Morrison shows these two faults as cutting Kansan(?) alluvium (early middle Pleistocene). The scarps have not been measured, but their subdued morphology suggests late, rather than latest, Pleistocene movement.

WASHBURN RANCH FAULT ZONE (9)

The Washburn Ranch fault zone forms fresh-appearing scarps along the west margin of the central part of the Animas Valley. The scarps face east and extend nearly 15 km, from near the latitude of Cowboy Pass to just south of New Mexico State Highway 9, west of Animas, N. Mex. Washburn Ranch is near the north end of the fault zone.

The faults were first mapped and briefly described by Gillerman (1958), who noted that the fault scarps are incompletely buried by deposits along intermittent streams. He judged, therefore, that some of the displacement was Holocene. Drewes and Thorman (1980b) identified several additional scarps along the fault zone and showed their exact location, but did not discuss their age.

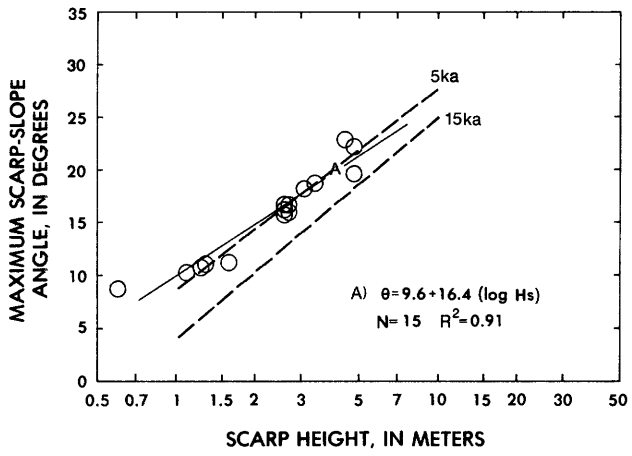

Figure 8.--Maximum scarp-slope angle (θ) plotted against scarp height (Hs) for the northern part of the Washburn fault zone (fault 9 on accompanying map).

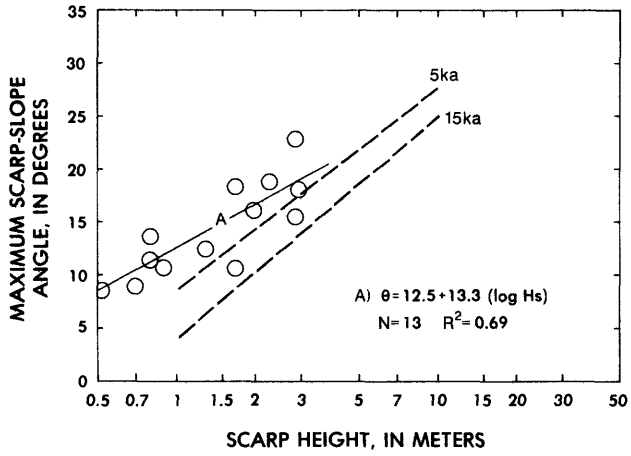

Figure 9.--Maximum scarp-slope angle (θ) plotted against scarp height (Hs) for the southern part of the Washburn fault zone (fault 9 on accompanying map).

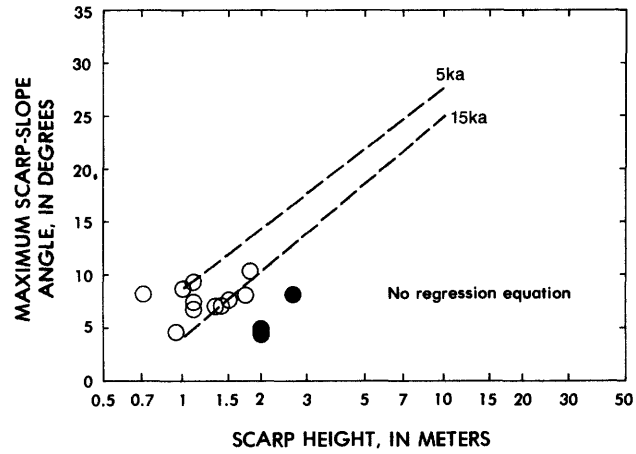

Figure 10.--Maximum scarp-slope angle (θ) plotted against scarp heights (Hs and Hm) for the Animas Valley fault (fault 10 on the accompanying map). Open circles are for most recent single-event part of scarp; filled circles are for entire multiple-event scarp.

Scarps of the Washburn Ranch fault zone are 0.5-5 m high on middle Pleistocene to Holocene(?) fan alluvium. The presence of scarps of comparable height on alluvium of such varying ages suggests that the faulting occurred during a single, fairly recent episode. Scarp morphology data from the northern and southern parts of the fault (figs. 8 and 9, respectively) support Gillerman's inferred Holocene age of faulting. The stratigraphic and morphologic data indicate scarps along the Washburn Ranch fault zone are some of the youngest in the map area. Additionally, the fault is aligned with basalt vents and cuts basalt flows that have been dated at 0.14-0.54 Ma (table 1).

ANIMAS VALLEY FAULT (10)

The Animas Valley fault is marked by west-facing scarps that extend 19 km along the western piedmont of the Pyramid Mountains, northeast of Cotton City, N. Mex. Reeder (1957) mentioned young faulting in this area, and Gillerman (1958) also briefly mentioned young faulting northeast of Cotton City. Smith (1978) informally used the name "Animas Valley fault" to describe the young faulting northeast of Cotton City, and Thorman and Drewes (1978) showed the northern part of the faults on their map. S. G. Wells (in Elston and others, 1983, p. 17) briefly discussed the Quaternary deposits and the Animas Valley fault in a report on the geothermal potential of this region.

The Animas Valley fault has a sinuous trace 1-5 km west of the Pyramid Mountains. Wells (in Elston and others, 1983) states that the scarps have as much as 5 m of vertical relief on thin piedmont-fan deposits having "well-developed" soil horizons. According to Wells, the youngest fault movement occurred in late Pleistocene or early Holocene time. Our scarp-profile data (fig. 10) collected along most of the length of the fault show less than 2 m of offset and maximum scarp-slope angles of 4°-8°. The morphologies of the 2-m-high scarps suggest multiple movement, and at least one compound scarp is identified in the central part of the fault. The Animas Valley fault cuts middle(?) to upper Pleistocene alluvium, but is buried by Holocene alluvium. Our data suggest that the most recent movement on the Animas Valley fault probably occurred in the latest Pleistocene.

Older, more subdued and dissected fault scarps less than 5 m high are found to the east, along the west front of the Pyramid Mountains (near the mouth of Jose Placencia Canyon). Although the morphology and degree of dissection of the scarps suggest that they are older than the Animas Valley fault (latest Pleistocene), they may be of late Pleistocene age.

GOLD HILL FAULT ZONE (11)

The Gold Hill fault zone is marked by discontinuous, en echelon, southwest-facing scarps along the southwestern flank of the southern part of the Big Burro Mountains, 16 km northeast of Lordsburg, N. Mex. Our map of the fault scarps is a modified version of the maps by Hedlund (1978b) and by Drewes and others (1982). We found evidence of multiple fault movements dating from middle to late Pleistocene. The scarps at the north end of the fault zone are formed on middle and upper Pleistocene alluvium, but are buried by Holocene alluvium. The stratigraphic evidence shows that the youngest move-

ment occurred in late Pleistocene time. Scarp heights are about 9 m on middle Pleistocene alluvium and about 6 m on adjacent upper Pleistocene alluvium, indicating probable recurrent faulting.

Near the mouth of Gold Hill Canyon, a very subdued scarp is preserved on middle(?) to upper Pleistocene alluvium, but is buried by uppermost Pleistocene and Holocene alluvium. Scarp heights of 2 m and scarp-slope angles of 5° suggest a late Pleistocene age for the scarp.

MANGAS FAULT (12)

The Mangas fault forms a steep, linear escarpment along the southwestern flank of the Little Burro Mountains, just east of Tyrone, N. Mex. The fault is the southernmost of several faults that form the eastern margin of the Mangas graben, which extends north of the map area. Paige (1922) first mapped the Mangas fault during a study of the Tyrone copper district. Gillerman (1964, p. 26) noted that an "eroded fault scarp" marked the surface trace of the fault and that the fault places the Gila Conglomerate against bedrock of the Little Burro Mountains. Gillerman suggested Quaternary movement on the fault, although he had no direct evidence to support this inference. Recent detailed mapping in the area (Hedlund, 1978a, 1978c) shows that the Mangas fault is concealed by alluvium of unknown age along the entire southwest side of the Little Burro Mountains.

We find that Pleistocene alluvium, which unconformably overlies the Gila Conglomerate in this area, is not displaced by the Mangas fault, but that the Gila Conglomerate has been downfaulted and rotated against bedrock. However, near the northwest end of the Little Burro Mountains, Pliocene(?) basalt interbedded in the upper part of the Gila Conglomerate appears to have been offset little (or not at all) where it straddles the Mangas fault. By this evidence the Mangas fault may have had Pliocene movement, but not Pleistocene movement.

NORTH SWISSHELM FAULT (13)

The North Swisshelm fault, which forms a prominent, high escarpment along the northeast side of the Swisshelm Mountains about 40 km north of Douglas, Ariz., has been studied in detail by Druke (1979). The northwest projection of the escarpment lines up with the northeastern edge of the Squaretop Hills and coincides with a high-angle normal fault exposed at the northernmost end of the Swisshelm Mountains. The escarpment is 20-60 m high and is as steep as 30°, suggesting a history of fairly recent and episodic movement. However, interpretation of the scarp's morphology is complicated by fluvial cutting along Whitewater Draw, which has clearly eroded the base and steepened the scarp along much of its length. Maximum scarp-slope angles decrease to 14° away from Whitewater Draw. Upper Pleistocene and younger terrace alluvium is not offset by the fault. On the basis of cross-cutting relations, analysis of maximum scarp-slope angle versus scarp height, and the width of the zone of crestal rounding, Druke (1979) concluded that the fault was most recently active during the early to early middle Pleistocene (2.0-0.5 Ma).

SOUTH SWISSHELM FAULT (14)

The South Swisshelm fault is along the southeastern margin of the Swisshelm Mountains, 30 km north of Douglas, Ariz. The fault strikes northwest, dips 60°-70° eastward, and, in several exposures, places lower to upper Miocene tuffaceous basin-fill deposits against Paleozoic sedimentary rocks of the Swisshelm mountain block. Late Cenozoic movement is suggested by the straightness of the mountain front, although at least some of this linearity is controlled by resistant, east-dipping Paleozoic rocks that strike nearly parallel to the range front. Several 20-m-high discontinuous escarpments are formed on dissected lower Pleistocene to lower tuffaceous basin-fill deposits against Paleozoic sedimentary rocks of the Swisshelm mountain block. Late Cenozoic movement is suggested by the straightness of the mountain front, although at least some of this linearity is controlled by resistant, east-dipping Paleozoic rocks that strike nearly parallel to the range front. Several 20-m-high discontinuous escarpments are formed on dissected lower Pleistocene to lower middle Pleistocene alluvium along the projection of the fault. The most recent movement along the fault is thought to be no younger than middle Pleistocene, on the basis of the presence of undisturbed upper middle Pleistocene to upper Pleistocene alluvium that buries the fault at several places.

FAULTS OF THE SAN BERNARDINO VALLEY (15, 16, 18, 19, 22)

Much of the evidence of faulting in the San Bernardino Valley is either buried by, or manifested in, Pliocene and Pleistocene basalt. Basalt of the San Bernardino volcanic field (Lynch, 1972, 1978) is subdivided into three general age groups: (1) mesa-capping basalt about 3 Ma that forms dissected remnants perched on ridges surrounding the San Bernardino Valley, (2) basalt (0.3-1.0 Ma) of the main volcanic field, exposed only within the modern valley, and (3) a series of basalt flows of undetermined (but probably intermediate) age that locally have flowed over basin-margin escarpments 140-400 m high. These escarpments structurally separate the older and younger basalt. Several characteristics of these high escarpments, including their relation to the various basalt flows and their straightness, strongly suggest they were formed by faulting after deposition of the 3-Ma basalt.

A prominent escarpment on the west side of the San Bernardino Valley is here named the "Pedregosa fault" (16). The fault corresponds to parts of the Buck Creek and Perilla faults mapped by Drewes (1980). An escarpment 10 km long on the east side of the valley is here named the "Outlaw Mountain fault zone" (18). The Pedregosa fault and the Outlaw Mountain fault zone generally trend north and define a broad graben. Hayes' (1982) map shows that parts of the Outlaw Mountain fault zone cut Pliocene(?) to Pleistocene basalt. On the basis of the concept that tectonically active mountain ranges have steep and straight mountain fronts (Bull, 1973), we interpret the slightly sinuous and embayed margins of the San Bernadino Valley as suggesting that recent rates of uplift are low along the bounding faults.

The Guadalupe Canyon fault (22) strikes nearly east-west in the southeastern part of the Peloncillo Mountains, about 45 km east of Douglas, Ariz., and just 1-2 km north of the international boundary with Mexico. Hayes (1982) showed the fault as displacing mainly Cretaceous and Oligocene rocks, although Pliocene to Pleistocene (1-3 Ma?) basalt is in contact with the fault in at least one place. The fault has down-to-the-south displacement in bedrock. Our observations show that the fault forms scarps 10-20 m high that extend but 3 km across a thin veneer of Pliocene to lower Pleistocene alluvium. We have no evidence, other than the presence of fault scarps, that the last movement on the fault is substantially younger than the alluvium that it cuts.

The only fault scarp we found on alluvium in the San Bernadino Valley is along the central part of the Pedregosa fault, 2 km northwest of Bernardino Station. The scarp is 15-20 m high on lower(?) to middle Pleistocene alluvium. The faulted deposits lie on a broad east-sloping pediment. Directly to the south, an undated basalt flow tentatively correlated with the youngest basalt of the field (1.0-0.3 Ma) crosses the south end of the Pedregosa fault but is undisturbed.

No unequivocal fault scarps were found within the interior of the volcanic field, although strong linear alignment of vents suggests that they are controlled by faults in the subsurface. Gravity surveys by Lynch (1972) further suggest that a series of north-trending faults are buried by the volcanic rocks of the San Bernardino Valley. Well data indicate that the graben of San Bernardino Valley contains at least 240 m of upper basin fill and several interbedded basalt flows (Lynch, 1972). Apparently, most of the faulting took place from 3 to 1 Ma, partly during (and perhaps genetically related to) the first phase of basalt extrusion in the volcanic field. The amounts and rates of tectonism, volcanism, and sedimentation have decreased markedly since the eruption of the young basalt flows that blanket the valley floor.

Times of movement on many other faults in the San Bernadino Valley--namely the Joe Glenn Ranch faults (15), the Bunk Robinson Peak fault zone (19), and the Guadalupe Canyon fault (22)--are not well dated, but movement on these faults may have accompanied or closely followed eruption of the 3-Ma basalt. These faults are distributed over a wide area (Cooper, 1959; Hayes, 1982), they trend in various directions (north-south to east-west), and they thus have preceded the later tectonic activity in the San Bernardino Valley.

The relatively old movement on the faults contrasts with the recent faulting that accompanied the great earthquake of 1887 in nearby Sonora, Mexico (Sumner, 1977). Fault scarps formed during the earthquake are 1-5 m high and 75 km long and project north into the United States along the eastern margin of the San Bernardino Valley (Herd and McMasters, 1982). The north end of the scarps is about 8 km south of the international boundary with Mexico.

CHIRICAHUA FAULT (17)

The Chiricahua fault forms the eastern margin of the Chiricahua Mountains for 30 km from Portal, Ariz., to Apache, Ariz. Along the northern part of the fault there is undisturbed Holocene(?) alluvium, whereas lower(?) middle Pleistocene alluvium is offset a minimum of 3-5 m and upper(?) middle Pleistocene alluvium is offset 1-3 m. The morphology of the smaller scarps indicates that the latest movement on the Chiricahua fault was in Holocene time (fig. 11). At least one earlier movement, implied by greater offset of adjacent lower(?) middle Pleistocene alluvium, probably occurred more than 200 ka.

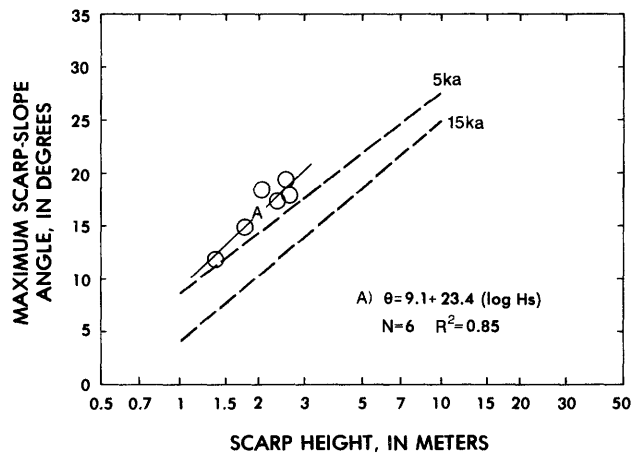

Figure 11.--Maximum scarp-slope angle (θ) plotted against scarp height (Hs) for the Chiricahua fault (fault 17 on the accompanying map).

Farther south, the eastern front of the Chiricahua Mountains becomes abrupt and fairly straight, abutted by extensive young alluvial fans. Such features may be evidence of relatively recent uplift along a range-bounding fault (Bull, 1973). However, we have not seen the Chiricahua fault in this area and have no personal knowledge of its age.

GRAYS RANCH FAULT ZONE (20)

The Grays Ranch fault zone forms the east boundary of the south-central Peloncillo Mountains, which face the lower Animas Valley (Wrucke and Bromfield, 1961). A series of east-facing escarpments marks the trace of the fault zone, from just south of Big Creek, south 16 km nearly to the confluence of Indian and Animas Creeks. Pliocene(?) to lower(?) Pleistocene alluvium is faulted against middle Tertiary volcanic rock along the northern and southern parts of the fault. Quaternary movement along these parts of the fault is suggested by straight, well-defined escarpments that contrast with the embayed character of the rest of the Peloncillo mountain front. Along the central part of the fault zone, a distinct fault scarp 10-15 m high is formed on lower to middle Pleistocene piedmont-slope alluvium that overlies an uplifted pediment. Although the time of last movement is poorly determined, the subdued morphology of the fault scarp and the presence of undisturbed middle(?) to upper Pleistocene alluvium to the south suggests that the most recent movement is probably no younger than middle Pleistocene.

GILLESPIE MOUNTAIN FAULT (21)

The Gillespie Mountain fault forms the northwestern margin of the Animas Mountains, from Animas Peak northward about 25 km as originally mapped by Zeller (1962), and later by Zeller and Alper (1965). Our observations at the northern end of the fault show upper Pleistocene alluvium is offset 1-3 m and lower Pleistocene to lower middle Pleistocene alluvium is offset 8-13 m, whereas upper Holocene terrace alluvium is undisturbed. The older alluvium lies on an uplifted and dissected Quaternary pediment. Uplift and dissection of the pediment implies that recurrent Quaternary movement occurred after an extensive period of tectonic quiescence during which the pediment was formed. The morphology of the scarps indicates that the most recent movement along the fault occurred in Holocene time (fig. 12). However, we are not certain how far south Holocene movement can be recognized.

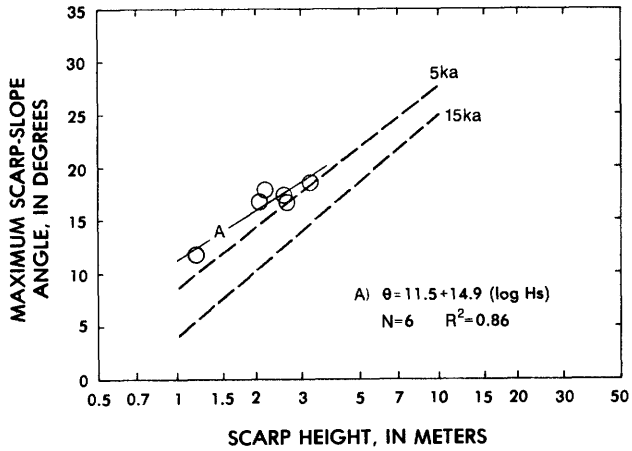

Figure 12.--Maximum scarp-slope angle (θ) plotted against scarp height (Hs) for the Gillespie Mountain fault (fault 21 on the accompanying map).

SUMMARY AND CONCLUSIONS

Quaternary and Pliocene faults are common along part of the east and west sides of mountain ranges in the Rio Grande rift and Basin and Range Province in southeastern Arizona and southwestern New Mexico. The faults trend mainly north-south, except in the northern part of the area, where they trend northwest. Most of the faults displace Pleistocene and, in places, Holocene surficial deposits, Pliocene to Pleistocene basalt, and Pliocene to lower(?) Pleistocene basin-fill deposits. Soils and geomorphic and geologic data collected along some of the major scarps indicate that many of the resulting scarps formed during the late Pleistocene, and some as recently as the Holocene.

The most recent faulting in the general region occurred in historic time (1887 A.D.) along the east side of the San Bernardino Valley where it extends into northern Mexico, 8 km south of the map area. Prehistoric movement is recorded by many young fault scarps in Pliocene and Quaternary deposits. Our morphologic data suggest that six of the faults and(or) fault zones had significant movement in Holocene ($\leq$10 ka) or latest Pleistocene (10-25 ka) time. In the northern part of the map area, both the North Safford (3) and the South Safford (4) fault zones were active during this time. In the southern part of the map area, movement occurred on the Washburn Ranch (9) fault zone, the Animas Valley fault (10), and the Gillespie Mountain (21) fault, all of which bound the Animas Valley, N. Mex., and the Chiricahua (17) fault, which bounds the west margin of the southern part of the San Simon Valley, Ariz.

Faults and fault zones having evidence of lastest movement in the late Pleistocene (25-150 ka) include the Rimrock fault (7) and possibly the Buena Vista fault (2) (both in the northern part of the map area), and the Animas Valley (10) and Gold Hill (11) faults (both in the central part of the map area). Scarps may have formed as late as the middle Pleistocene on the Ward Canyon fault (5) (at the north edge of the map area) and on the South Swisshelm (14) and Pedregosa (16) faults and along segments of the Grays Ranch fault zone (20) (all in the south-central part of the map area). Faults whose latest movement is Pliocene or early Pleistocene include the Maverick Hill (6) fault (in the northern part of the map area) and most faults associated with the San Bernardino volcanic field (Joe Glenn Ranch faults, 15; Outlaw Mountain fault zone, 18; Bunk Robinson Peak fault zone, 19; and Guadalupe Canyon fault, 22).

The amount of offset recorded by fault scarps in the area depends upon the number of movements and age of the deposit on which the scarp is formed. The large scarps on lower to middle Pleistocene surficial deposits along the Gillespie Mountain (21) and Rimrock (7) faults are as much as 13 m and 17 m in height, respectively. Scarps 20 m or more in height are on lower Pleistocene deposits along the Ward Canyon (5), Maverick Hill (6), South Swisshelm (14), Joe Glenn Ranch (15), and Pedregosa (16) faults. Fault scarps this large are usually the result of recurrent movement, as evidenced by increasing amounts of displacement in progressively older deposits. In addition, steep escarpments 50 m or greater in height are formed on Pliocene and lower Pleistocene deposits along the Mangas (12), North Swisshelm (13), and Pedregosa (16) faults, and the Outlaw Mountain (18) and Bunk Robinson Peak (19) fault zones. Although created by faulting, some of the relief of the escarpments (fault-line scarps) is the result of erosion, and thus height is not an accurate measure of the offset on the faults.

Despite the relative abundance of young faults in the area, very little is known about their Quaternary and Pliocene slip rates. Dated basalt flows that are offset along the Washburn Ranch fault zone indicate a late Quaternary slip rate of 5-20 m/Ma, which is low compared to the slip rates along some major range-bounding faults in parts of the Rio Grande rift (Machette and McGimsey, 1983) in central New Mexico. However, low slip rates might be expected for the Washburn Ranch fault zone because the measurements were made near the southern terminus, rather than near the middle of the zone. In the San Bernardino Valley, 3-Ma basalt flows are uplifted on both flanks of the valley, but are covered completely by younger flows on the downthrown sides of the Pedregosa (16) fault and the Outlaw Mountain (18) fault zone. The topographic relief along these escarpments is as much as 400 m. If this relief is strictly a result of faulting, the minimum vertical slip rate has been 130-400 m/Ma during the past 1-3 Ma. However, much of the faulting in this part of the San Bernardino Valley appears to have been local and related to volcanic activity between 3 and 1 Ma, so these slip rates may not apply to the last half of the Quaternary.

Some of the fault scarps in the area are along basin-bounding faults that lie at the upper margins of pediments. This relation suggests late Pliocene to Pleistocene reactivation of earlier Basin-and-Range-style normal faults, following either an early Pliocene tectonic lull (that is, geomorphic stability) or a drastic decrease in slip rate. In addition, most of the late Pleistocene faulting and most Pliocene-Pleistocene volcanic rocks in the region are along the margins of the Animas, San Simon, and San Bernardino Valleys, in the southern part of the map area. This distribution may indicate either (1) a spatially restricted young pulse of tectonic activity, or (2) activation of a different neotectonic regime, perhaps with the formation of discrete, but small, extensional systems at the transition between the Basin and Range Province and the Rio Grande rift (Seager and Morgan, 1979).

The young faults shown on the accompanying map all have significant amounts of offset, and as such are probably related to prehistoric earthquakes of large magnitude (M>6). Considering the distribution, size, and number of faults that could have histories of recurrent movement in the map area, we conclude that there may have been hundreds of large-magnitude earthquakes associated with surface ruptures during Pliocene and Quaternary time. Pearthree and others (1983) showed that the composite recurrence interval for Quaternary faulting in southeastern Arizona (the western part of the map area) is 10^5 yr/event. In the south-central part of the map area, which appears to have a concentration of latest Pleistocene and Holocene faults, the interval is probably about 10^4 yr/event. The latter recurrence interval is comparable to that in the Basin and Range Province of northwestern Arizona (10^4 yr/event, Pearthree and others, 1983) and slightly longer than in the Rio Grande rift in central New Mexico (10^3–10^4 yr/event; Machette and McGimsey, 1983).

Table 3.--Morphology data for some fault scarps in the map area

[Symbols: θ, maximum scarp-slope angle; Hs, height of single-event scarp; Hm, height of multiple-event scarp; *, data not used in regression equation; ---, not determined; n, number of data pairs; R^2, coefficient of determination. Regression equations shown for lines of best fit]

No.	θ (degrees)	Hs (m)	Hm (m)	Remarks
North Safford fault zone (3), latest Pleistocene (Scarp data collected by Pearthree and Calvo; data plotted in figure 6)				
p3-1	10.6	3.8	5.3	Compound scarp.
p3-2	10.7	3.3	4.9	Do.
p3-3	12.1	3.3	4.3	Do.
p3-4	14.3	3.2	4.7	Do.
p3-5	9.0	1.2	---	
p3-6	6.9	1.8	---	
p3-8	6.4	1.7	---	
p3-9	6.1	1.8	---	
p3-10	21.5	5.0	9.5	Compound scarp.
p3-11	17.6	5.3	7.3	Do.
p3-12	22.3	6.0	---	
p3-14	21.3	6.7	---	
p3-17	13.9	3.7	---	
p3-18	11.4	3.3	---	
p3-19	14.1	2.8	---	
p3-20	15.0	2.8	---	
p3-21	15.5	3.7	---	
p3-23	15.9	3.1	4.1	Compound scarp.
p3-24	7.5	1.4	---	
p3-25	9.7	2.2	---	
Regression equation: θ=3.1+21.1(log Hs), n=20, R^2=0.76.				
South Safford fault zone (4), Holocene(?) (Scarp data collected by Pearthree and Calvo; data shown in figure 7)				
p4-1	3.0	1.5	---	
p4-2	6.5	2.8	3.5	Compound scarp.
p4-3	5.0	2.1	---	
p4-4	5.1	2.7	---	
p4-5	5.0	1.4	---	
p4-6	4.0	1.1	---	
p4-7	5.0	1.7	---	
p4-8	5.4	2.1	---	
p4-9	5.1	2.8	---	
p4-10	10.0	3.3	4.4	Compound scarp.
p4-11	4.3	1.3	---	
p4-12	11.0	2.7	3.5	Compound scarp.
p4-13	10.4	2.3	3.6	Do.
p4-15	7.5	2.9	---	
p4-16	6.4	1.7	---	
p4-17	4.1	.7	---	
p4-18	4.7	1.2	---	
p4-19	5.0	.7	---	
Regression equation: θ=4.3+6.7(log Hs), n=18, R^2=0.36.				
Washburn Ranch fault zone (9), Holocene (Scarp data collected by Machette along northern part shown in figure 8; data collected by Pearthree and Menges along southern part shown in figure 9)				
Northern part:				
m15-1	22.75	4.4	---	
m15-2	16.0	2.6	---	
m15-3	10.5	1.25	---	
m15-4	10.75	1.3	---	
m15-5	16.5	2.7	---	
m15-6a	8.5	.6	---	Splay
m15-6b	11.0	1.6	---	Splay
m15-7	19.5	4.8	---	
m15-8	22.0	4.8	---	
m15-9	18.0	3.1	---	
m15-10	15.8	2.7	---	
m15-11	15.5	2.6	---	
m15-12	10.0	1.1	---	
m15-13	16.5	2.6	---	
m15-14	18.5	2.9	---	
Regression equation: θ=9.6+16.4(log Hs), n=15, R^2=0.91.				
Southern part:				
p9-1	10.8	1.7	---	
p9-2	18.5	1.7	---	
p9-3	19.0	2.3	---	
p9-4	18.2	3.0	---	
p9-5a	9.0	.7	---	Splay
p9-5b	8.0	.4	---	Splay
p9-6	10.8	.9	---	
p9-7	16.2	2.0	---	
p9-8	15.8	2.9	---	
p9-9	13.8	.8	---	
p9-10	23.0	2.9	---	
p9-11	11.5	.8	---	
p9-12	12.5	1.3	---	
Regression equation: θ=12.5+13.3(log Hs), n=13, R^2=0.69.				

Note: Table 3 is continued on next page.

Table 3.--Morphology data for some fault scarps in the map area--Continued

No.	θ (degrees)	Hs (m)	Hm (m)	Remarks
Animas Valley fault (10), latest Pleistocene (Scarp data collected by Machette (M) and Pearthree and Menges (PM); data shown in figure 10)				
m28-1	4.8	---	2.0	M, compound(?) scarp.
m28-2	4.25	0.9	2.0	Do.
m28-3	8.0	1.75	2.65	M
m28-4	7.0	1.35	---	M
p10-1	9.25	1.1	---	PM
p10-2	7.0	1.4	---	PM
p10-3	7.25	1.1	---	PM
p10-4	7.5	1.5	---	PM
p10-5	6.75	1.1	---	PM
p10-6	7.0	1.5	---	PM
p10-7	8.0	.7	---	PM
p10-8	10.25	1.8	---	PM
p10-9	8.5	1.0	---	PM
No regression equation.				
Gold Hill fault zone (11), late Pleistocene (Scarp data collected by Machette)				
m29-1	5.0	2.2	---	
m29-2	5.75	---	5.9	Compound scarp.
m29-3	10.4	4.7	8.5	Compound scarp, Hs is approximate.
No regression equation.				
Chiricauhua fault (17), Holocene (Scarp data collected by Pearthree and Menges; data shown in figure 11)				
p17-1	12.0	1.4	---	
p17-2	18.0	2.7	---	
p17-3	17.5	2.4	---	
p17-4	15.0	1.8	---	
p17-5	18.5	2.1	---	
p17-6	19.5	2.6	---	
Regression equation: $\theta=9.1+23.4(\log Hs)$, $n=6$, $R^2=0.85$.				
Gillespie Mountain fault (21), Holocene (Scarp data collected by Pearthree and Menges; data shown in figure 12)				
p21-1	18.0	2.2	---	
p21-2	17.0	2.1	---	
p21-3	17.0	2.7	---	
p21-4	12.0	1.2	---	
p21-5	18.75	3.3	---	
p21-6	17.5	2.6	---	
Regression equation: $\theta=11.5+14.9(\log Hs)$, $n=6$, $R^2=0.86$.				

REFERENCES CITED

Aiken, C. L. V., 1978, Gravity and aeromagnetic anomalies of southeastern Arizona, in Callender, J. F., Wilt, J. C., and Clemons, R. E, eds., Guidebook of Land of Cochise, southeastern Arizona: New Mexico Geological Society, 29th Field Conference, p. 301-313.

Aiken, C. L. V., and Sumner, J. S., 1974, A geophysical and geological investigation of potentially favorable areas for petroleum exploration in southeastern Arizona: Arizona Oil and Gas Commission Report, no. 3, 40 p.

Aldrich, M. J., and Laughlin, A. W., 1982, Orientation of least-principal horizontal stress--Arizona, New Mexico, and the Trans-Pecos area of West Texas: Los Alamos National Laboratory Publication LA-9158-Map UC-11, scale 1:1,000,000.

Baldridge, W. S., Bartov, Y., and Kron, A., 1983, Geologic map of the Rio Grande rift and southeastern Colorado Plateau, New Mexico and Arizona, supplement to Riecker, R. E., ed., Rio Grande rift--tectonics and magmatism: Washington, D.C., American Geophysical Union, scale 1:500,000.

Birkeland, P. W., 1984, Soils and geomorphology: New York, Oxford University Press, 372 p.

Bucknam, R. C., 1980, Characteristics of active faults in the Great Basin, in Summaries of Technical Reports, v. 9, National Earthquake Hazards Reduction Program: U.S. Geological Survey Open-File Report 80-6, p. 94-95.

Bucknam, R. C., and Anderson, R. E., 1979, Estimation of fault-scarp ages from a scarp-height-slope-angle relationship: Geology, v. 7, no. 1, p. 11-14.

Bull, W. B., 1973, Local base-level processes in arid fluvial systems: Geological Society of America Abstracts with Programs, v. 5, no. 7, p. 562.

Callender, J. F., Wilt, J. C., and Clemons, R. E., editors, 1978, Guidebook of Land of Cochise, southeastern Arizona: New Mexico Geological Society, 29th Field Conference, 372 p.

Chapin, C. E., 1979, Evolution of the Rio Grande rift--a summary, in Riecker, R. E., ed., Rio Grande rift--tectonics and magmatism: Washington, D.C., American Geophysical Union, p. 1-5.

Chapin, C. E., and Seager, W. R., 1975, Evolution of the Rio Grande rift in the Socorro and Las Cruces areas, in Seager, W. R., Clemons, R. E., and Callender, J. F., eds., Guidebook of Las Cruces country: New Mexico Geological Society, 26th Field Conference, p. 297-321.

Coney, P. J., 1978, The plate tectonic setting of southeastern Arizona, in Callender, J. F., Wilt, J. C., and Clemons, R. E., eds., Guidebook of Land of Cochise, southeastern Arizona: New Mexico Geological Society, 29th Field Conference, p. 285-290.

Cooper, J. R., 1959, Reconnaissance geologic map of southeastern Cochise County, Arizona: U.S. Geological Survey Mineral Investigations Field Studies Map MF-213, scale 1:125,000.

Cunningham, J. E., 1979, Geologic map of the Clifton area, Arizona: Arizona Bureau of Geology and Mineral Technology, unpublished map, scale 1:24,000.

Damon, P. E., Shafiqullah, Muhammad, and Lynch, D. J., 1973, Geochronology of block faulting and basin subsidence in Arizona: Geological Society of America Abstracts with Programs, v. 5, no. 7, p. 590.

Dane, C. H., and Bachman, G. O., 1961, Preliminary geologic map of the southwestern part of New Mexico: U.S. Geological Survey Miscellaneous Geologic Investigations Map I-344, scale 1:380,160.

Davis, G. H., 1979, Laramide folding and faulting in southeastern Arizona: American Journal of Science, v. 279, p. 543-569.

_____1981, Regional strain analysis of the superposed deformations in southeastern Arizona and the eastern Great Basin, in Dickenson, W. R., and Payne, W. D., eds., Relations of tectonics to ore deposits in the southern Cordillera: Arizona Geological Society Digest, v. 14, p. 155-172.

Deal, E. G., Elston, W. E., Erb, E. E., Peterson, S. L., Reiter, D. E., Damon, P. E., and Shafiqullah, Mohammad, 1978, Cenozoic volcanic geology of the Basin and Range Province in Hidalgo County, southwestern New Mexico, in Callender, J. F., Wilt, J. C., and Clemons, R. E., eds., Guidebook of Land of Cochise, southeastern Arizona: New Mexico Geological Society, 29th Field Conference, p. 219-229.

Dickson, J. J., and Izett, G. A., 1981, Fission-track ages of air-fall tuffs in Pliocene basin-fill sediments near 111 Ranch, Graham County, Arizona: Isochron/West, no. 32, p. 13-15.

Drewes, Harald, 1978, The Cordilleran orogenic belt between Nevada and Chihuahua: Geological Society of America Bulletin, v. 89, p. 641-657.

_____1980, Tectonic map of southeast Arizona: U.S. Geological Survey Miscellaneous Investigations Series Map I-1109, scale 1:125,000.

_____1981, Tectonics of southeastern Arizona: U.S. Geological Survey Professional Paper 1144, 96 p.

Drewes, Harald, and Thorman, C. H., 1980a, Geologic map of the Steins quadrangle and the adjacent part of the Vanar quadrangle, Hidalgo County, New Mexico: U.S. Geological Survey Miscellaneous Investigations Series Map I-1220, scale 1:24,000.

_____1980b, Geologic map of the Cotton City quadrangle and the adjacent part of the Vanar quadrangle, Hidalgo County, New Mexico: U.S. Geological Survey Miscellaneous Investigations Series Map I-1221, scale 1:24,000.

Drewes, Harald, Houser, B. B., Hedlund, D. C., Richter, D. H., Finnell, T. L., and Thorman, C. H., 1982, Geologic map of the Silver City 1°x2° quadrangle, New Mexico and Arizona: U.S. Geological Survey Miscellaneous Investigations Series Map I-1310-C, scale 1:250,000.

Druke, P. A., 1979, Geomorphology of the Swisshelm scarp, Cochise County, Arizona: Tucson, University of Arizona, M.S. thesis, 86 p.

Eberly, L. D., and Stanley, T. B., 1978, Cenozoic stratigraphy and geologic history of southwestern Arizona: Geological Society of America Bulletin, v. 89, no. 6, p. 921-940.

Elston, W. E., 1981, Mid-Tertiary extensional orogeny of southwestern New Mexico and other parts of the Basin and Range Province: U.S. Geological Survey Open-File Report 81-0503, p. 32-34.

Elston, W. E., Deal, E. G., and Logsdon, M. J., 1983, Geology and geothermal waters of the Lightning Dock region, Animas Valley and Pyramid Mountains, Higalgo County, New Mexico: New Mexico Bureau of Mines and Mineral Resources Circular 177, 44 p.

Elston, W. E., Rhodes, R. C., Coney, P. J., and Deal, E. G., 1976, Progress report on the Mogollon Plateau volcanic field, southwestern New Mexico--No. 3, surface expression of a pluton, in Elston, W. E., and Northrop, S. A., eds., Cenozoic volcanism in southwestern New Mexico: New Mexico Geological Society Special Publication, no. 5, p. 3-28.

Fitzsimmons, J. P., and Lochman-Balk, Christina, editors, 1965, Guidebook of southwestern New Mexico II: New Mexico Geological Society, 16th Field Conference, 244 p.

Gilbert, G. K., 1875, Report on the geology of portions of New Mexico and Arizona: U.S. Geographic and Geologic Survey west of the 100th meridian (Wheeler Survey), v. 3, p. 501-567.

Gillerman, Elliot, 1958, Geology of the central Peloncillo Mountains, Hidalgo County, New Mexico, and Cochise County, Arizona: New Mexico Bureau of Mines and Mineral Resources Bulletin 57, 152 p.

_____1964, Mineral deposits of western Grant County, New Mexico: New Mexico Bureau of Mines and Mineral Resources Bulletin 83, 213 p.

Hawley, J. W., compiler, 1978, Guidebook to the Rio Grande rift in New Mexico and Colorado: New Mexico Bureau of Mines and Mineral Resources Circular 163, 241 p.

Hayes, P. T., 1982, Geologic map of Bunk Robinson Peak and Whitmire Canyon roadless areas, Coronado National Forest, New Mexico and Arizona: U.S. Geological Survey Miscellaneous Field Studies Map MF-1425-A, scale 1:62,500.

Hedlund, D. C., 1978a, Geologic map of the Gold Hill quadrangle, Hidalgo and Grant Counties, New Mexico: U.S. Geological Survey Miscellaneous Field Studies Map MF-1035, scale 1:24,000.

_____1978b, Geologic map of the Wind Mountain quadrangle, Grant County, New Mexico: U.S. Geological Survey Miscellaneous Field Studies Map MF-1031, scale 1:24,000.

_____1978c, Geologic map of the Tyrone quadrangle, Grant County, New Mexico: U.S. Geological Survey Miscellaneous Field Studies Map MF-1037, scale 1:24,000.

Heindl, L. A., 1958, Cenozoic alluvial deposits of the upper Gila River area, New Mexico and Arizona: Tucson, University of Arizona, Ph.D. thesis, 249 p.

_____1962a, Cenozoic geology of Arizona--a 1960 resume: Arizona Geological Society Digest, v. 5, p. 9-24.

_____1962b, Should the term "Gila Conglomerate" be abandoned?: Arizona Geological Society Digest, v. 5, p. 73-88.

Herd, D. G., and McMasters, C. R., 1982, Surface faulting in the Sonora, Mexico earthquake of 1887: Geological Society of America Abstracts with Programs, v. 14, no. 4, p. 172.

Johnson, N. M., Opdyke, N. D., and Lindsay, E. H., 1975, Magnetic polarity stratigraphy of Pliocene-Pleistocene terrestrial deposits and vertebrate faunas, San Pedro Valley, Arizona: Geological Society of America Bulletin, v. 86, no. 1, p. 5-12.

Keith, S. B., and Reynolds, S. J., 1977, Compilation of radiometric age dates for Arizona: Arizona Bureau of Geology and Mineral Technology Open-File Report 77-1, 187 p., plate 1, scale 1:1,000,000.

Laughlin, A. W., Aldrich, M. J., and Vaniman, D. T., 1983, Tectonic implications of mid-Tertiary dikes in west-central New Mexico: Geology, v. 11, no. 1, p. 45-48.

Lindsay, E. H., 1978, Late Cenozoic vertebrate faunas, southeastern Arizona, in Callender, J. F., Wilt, J. C., and Clemons, R. E, eds., Guidebook of Land of Cochise, southeastern Arizona: New Mexico Geological Society, 29th Field Conference, p. 269-275.

Lipman, P. W., 1981, Volcano-tectonic setting of Teriary ore deposits, southern Rocky Mountains, in Dickinson, W. R., and Payne, W. D., eds., Relations of tectonics to ore deposits in the southern Cordillera: Arizona Geological Society Digest, v. 14, p. 199-213.

_____1983, Cenozoic magmatism associated with extensional tectonics in the Rocky Mountains: Geological Society of America Abstracts with Programs, v. 15, no. 5, p. 288.

Loring, A. K., 1976, The age of Basin and Range faulting in Arizona, in Wilt, J. C., and Jenny, J. P., eds, Tectonic digest: Arizona Geological Society Digest, v. 10, p. 229-257.

Lynch, D. J., 1972, Reconnaissance geology of the San Bernardino volcanic field, Cochise County, Arizona: Tucson, University of Arizona, M.S. thesis, 101 p.

_____1978, The San Bernardino volcanic field of southeastern Arizona, in Callender, J. F., Wilt, J. C., and Clemons, R. E., eds., Guidebook of Land of Cochise, southeastern Arizona: New Mexico Geological Society, 29th Field Conference, p. 261-268.

Machette, M. N., 1986, History of Quaternary offset and paleoseismicity along the La Jencia fault, central Rio Grande rift, New Mexico: Bulletin of the Seismological Society of America, v. 76, no. 1, p. 259-272.

Machette, M. N., and Colman, S. M., 1983, Age and distribution of Quaternary faults in the Rio Grande rift--evidence from morphometric analysis of fault scarps: Geological Society of America Abstracts with Programs, v. 15, no. 5, p. 320.

Machette, M. N., and McGimsey, R. G., 1983, Map of Quaternary and Pliocene faults in the Socorro and western part of the Fort Sumner 1°x2° quadrangles, central New Mexico: U.S. Geological Survey Miscellaneous Field Studies Map MF-1465-A, scale 1:250,000.

Marvin, R. F., and Cole, J. C., 1978, Radiometric ages--compilation A, U.S. Geological Survey: Isochron/West no. 22, p. 3-14.

Marvin, R. F., Naesar, C. W., and Mehnert, H. H., 1978, Tabulation of radiometric ages --including unpublished K-Ar and fission-track ages--for rocks in southeastern Arizona and southwestern New Mexico, in Callender, J. F., Wilt, J. C., and Clemons, R. E., eds., Guidebook of Land of Cochise, southeastern Arizona: New Mexico Geological Society, 29th Field Conference, p. 243-252.

McKee, E. H., and Anderson, C. E., 1971, Age and chemistry of Tertiary volcanic rocks in north-central Arizona and relation of the rocks to the Colorado Plateau: Geological Society of America Bulletin, v. 82, no. 10, p. 2767-2782.

Melton, M. A., 1965, The geomorphic and paleoclimatic significance of alluvial deposits in southern Arizona: Journal of Geology, v. 73, no. 1, p. 1-38.

Menges, C. M., 1981, The Sonoita Creek basin--implications for late Cenozoic tectonic evolution of basins and ranges in southeastern Arizona: Tucson, University of Arizona, M.S. thesis, 239 p.

Menges, C. M., Mayer, Larry, and Lynch, D. J., 1981, Tectonic significance of a post mid-Miocene stress rotation inferred from fault and volcanic vent orientations in the Basin and Range Province of southeastern Arizona and northern Sonora: Geological Society of America Abstracts with Program, v. 13, no. 2, p. 96.

Menges, C. M., and McFadden, L. D., 1981, Evidence for a latest Miocene to Pliocene transition from Basin and Range tectonic to post-tectonic landscape evolution in southeastern Arizona: Arizona Geological Society Digest, v. 13, p. 151-160.

Morrison, R. B., 1965, Geologic map of the Duncan and Canador Peak quadrangles, Arizona and New Mexico: U.S. Geological Survey Miscellaneous Geologic Investigations Map I-442, scale 1:48,000.

Nash, D. B., 1981, FAULT--A Fortran program for modelling the degradation of active normal fault scarps: Computers and Geosciences, v. 7, p. 249-266.

Paige, Sidney, 1922, Copper deposits of the Tyrone district, New Mexico: U.S. Geological Survey Professional Paper 122, 53 p.

Pearthree, P. A., Menges, C. M., and Mayer, Larry, 1983, Distribution, recurrence intervals, and estimated magnitudes of Quaternary faulting in Arizona: Geological Society of America Abstracts with Programs, v. 15, no. 5, p. 417.

Reeder, H. O., 1957, Groundwater in Animas Valley, Hidalgo County, New Mexico: New Mexico State Engineers Technical Report 11, 101 p.

Scarborough, R. B., 1975, Chemistry and age of late Cenozoic air-fall ashes in southeastern Arizona: Tucson, University of Arizona, M.S. thesis, 107 p.

Scarborough, R. B., and Pierce, H. W., 1978, Late Cenozoic basins of Arizona, in Callender, J. F., Wilt, J. C., and Clemons, R. E., eds., Guidebook of Land of Cochise, southeastern Arizona: New Mexico Geological Society, 29th Field Conference, p. 253-259.

Scott, W. R., McCoy, W. D., Shroba, R. R., and Rubin, Meyer, 1983, Reinterpretation of the exposed record of the last two cycles of Lake Bonneville, Western United States: Quaternary Research, v. 20 , no. 3, p. 261-285.

Seager, W. R., and Morgan, Paul, 1979, Rio Grande rift in southern New Mexico, west Texas, and northern Chihuahua, in Riecker, R. E., ed., Rio Grande rift--tectonics and magmatism: Washington D. C., American Geophysical Union, p. 87-106.

Seager, W. R., Shafiqullah, Mohammad, Hawley, J. W., and Marvin, R. F., 1984, New K-Ar dates from basalts and the evolution of the southern Rio Grande rift: Geological Society of America Bulletin, v. 95, no. 1, p. 87-99.

Shafiqullah, Mohammad, Damon, P. E., Lynch, D.J., Kuck, P. H., and Rehrig, W. A., 1978, Mid-Tertiary magmatism in southeastern Arizona, in Callender, J. F., Wilt, J. C., and Clemons, R. E., eds., Guidebook of Land of Cochise, southeastern Arizona: New Mexico Geological Society, 29th Field Conference, p. 231-241.

Shafiqullah, Mohammad, Damon, P. E., Lynch, D. J., Reynolds, S. J., Rehrig, W. A., and Raymond, R. H., 1980, K-Ar chronology and geologic history of southwestern Arizona and adjacent areas: Arizona Geological Society Digest, v. 12, p. 201-260.

Shafiqullah, Mohammad, Damon, P. E., and Pierce, H. W., 1976, Late Cenozoic tectonic development of Arizona Basin and Range Province: International Geologic Congress, 25th, Sydney, Australia, 1976, Abstracts, v. 1, p. 99.

Smith, Christian, 1978, Geophysics, geology and geothermal leasing status of the Lightning Dock KGRA, Animas Valley, New Mexico, in Callender, J. F., Wilt, J. C., and Clemons, R. E., eds., Guidebook of Land of Cochise, southeastern Arizona: New Mexico Geological Society, 29th Field Conference, p. 343-348.

Sumner, J. R., 1977, The Sonora earthquake of 1877: Bulletin of the Seismological Society of America, v. 67, no. 4, p. 1219-1223.

Suneson, N. H., and Luchitta, Ivo, 1983, Origin of bimodal volcanism, southern Basin and Range Province, west-central Arizona: Geological Society of America Bulletin, v. 94, no. 8, p. 1005-1019.

Swan, M. M., 1976, The Stockton Pass fault--an element of the Texas lineament: Tucson, University of Arizona, M.S. thesis, 119 p.

Thorman, C. H., and Drewes, Harald, 1978, Geologic map of the Gary and Lordsburg quadrangles, Hidalgo County, New Mexico: U.S. Geological Survey Miscellaneous Investigations Series Map I-1151, scale 1:24,000.

Wallace, R. E., 1977, Profiles and ages of young fault scarps, north-central Nevada: Geological Society of America Bulletin, v. 88, no. 9, p. 1267-1281.

Witcher, J. C., 1980, Heat flow and the thermal regime in the Clifton, Arizona, area: Arizona Bureau of Geology and Mineral Technology Open-File Report 80-1a, 80 p.

Woodward, L. A., Callendar, J. F., and Zilinski, R. E., 1975, Tectonic map of the Rio Grande rift, New Mexico: Geological Society of America Map and Chart Series MC-11, scale 1:500,000.

Wrucke, C. T., and Bromfield, C. S., 1961, Reconnaissance geologic map of part of the southern Peloncillo Mountains, Hidalgo County, New Mexico: U.S. Geological Survey Mineral Investigations Field Studies Map MF-160, scale 1:62,500.

Zeller, R. A., Jr., 1962, Reconnaissance geologic map of the southern Animas Mountains: New Mexico Bureau of Mines and Mineral Resources Geologic Map 17, scale 1;62,500.

Zeller, R. A., Jr., and Alper, A. M., 1965, Geology of the Walnut Wells quadrangle, Hidalgo County, New Mexico: New Mexico Bureau of Mines and Mineral Resources Bulletin 84, 79 p.

Zoback, M. L., Anderson, R. E., and Thompson, G. A., 1981, Cainozoic evolution of the state of stress and style of tectonism of the Basin and Range Province of the Western United States: Philosophical Transactions of the Royal Society of London, series A, v. 300, p. 407-434.

Zoback, M. L., and Zoback, Mark, 1980, State of stress in the conterminous United States: Journal of Geophysical Research, v. 85, B11, p. 6113-6156.